

## COMPUTATIONAL SIMULATIONS OF SHOCK WAVE / LAMINAR BOUNDARY LAYER INTERACTION

Hasan Avsar<sup>1</sup>, Ali At<sup>2</sup> and Bayram Celik  
Istanbul Technical University, Istanbul, Turkey

### ABSTRACT

The main objective of this study is to understand better the interaction mechanism between a shock wave and a laminar boundary layer. A shock generator and a compression corner are used to create the desired shock waves. The interaction point of the shock wave and the boundary layer formed on a flat plate is designed in such a way that the flow is laminar at the interaction point. The angle between the flat plate and the incident shock wave is changed systematically to simulate the interaction mechanism and the flow characteristics for free stream Mach number of 2.15. 2-dimensional computational simulation results are evaluated in terms of the size, number and location of separation bubble/s; skin friction and pressure variation along the wall. As the deflection angle increases, additional separation bubbles are observed in the boundary layer which may cause 3-dimensional and/or unsteady flow.

### INTRODUCTION

When a supersonic flow is turned into itself as observed in the case of a compression corner, an oblique shock wave occurs. While the pressure, density, and temperature increase, Mach number and total pressure decrease discontinuously across the shock wave. Formation of an oblique shock wave at a concave corner or impingement of it on a wall causes a pressure rise in the vicinity of incidence point. As the shock-wave enters a boundary layer, its strength decreases continuously, and it becomes a Mach line on a streamline, where the flow is sonic. As a result of the pressure rise (adverse pressure gradient), the boundary layer thickens gradually up to the incidence point, and then thins rapidly again. This mechanism can result in separation and reattachment of the boundary layer locally. For example, in the case of impingement of an oblique shock wave on a laminar boundary layer that is formed on a flat plate, two distinct reflected shock waves occur upstream and downstream of the impingement point. The two reflected shock waves are generated by coalescence of the compression waves as a result of thickening boundary layer. In addition to the reflected shock waves, a Prandtl-Meyer expansion fan takes place downstream of the impingement point because of thinning boundary layer which turns the flow away from itself (see Figure 1) [Hughton and Carpante, 2012].

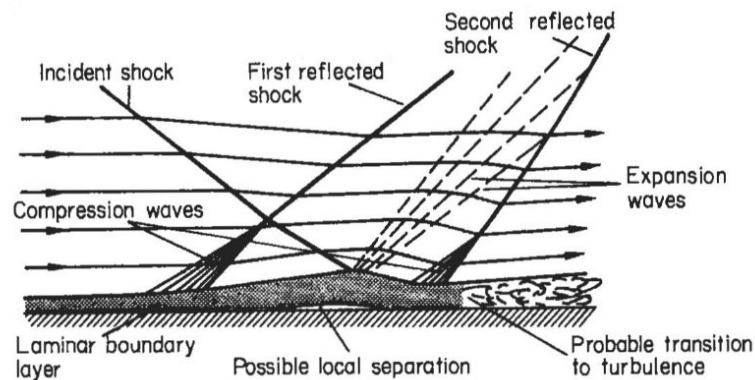


Figure 1: Shock wave laminar boundary layer interaction (SWBLI) [Houghton et al., 2012]

<sup>1</sup> Master Student in Department of Aeronautics and Astronautics Engineering, E-mail: avsarhas@itu.edu.tr

<sup>2</sup> Master Student in Department of Aeronautics and Astronautics Engineering, E-mail: at@itu.edu.tr

The interaction mechanism between a shock wave and a boundary layer is highly dependent on the upstream Mach number, shock impingement angle, and the type of the boundary layer. The length of the interaction region for turbulent flow is considerably shorter than the one for the laminar flow. This observation is because of relatively higher momentum of the particles near the wall in the case of turbulent flow, where the particles can overcome a greater adverse pressure gradient easily [Bertin, 2008]. Another discrepancy between the laminar and turbulent flow is turbulent boundary layer has a relatively thinner subsonic portion, where the propagation of shock-induced pressure to the upstream is limited.

It is known that the shock-wave/boundary layer interaction has a great influence on the pressure, shear stress, and heat-transfer distributions along the wall. Especially at hypersonic speed, the local heat-transfer rate at the reattachment point can reach a value that is an order of magnitude higher than those at the neighboring points [Anderson, 2011]

Although, there are numbers of theoretical and experimental studies on SWBLI [Holden, 2006], the computational studies are still limited [Bono, 2008; Degrez, 1987; Pirozzoli, 2009; Boin, 2006]. The interactions of different type of waves such as shocks, expansion, and compression, as well as the boundary layer in a very short distance make SWBLI a challenging problem. The solution of this problem requires a numerical schemes that is robust enough to withstand the rapid variations in the flow field while preserving the computational accuracy [Delery, 2000].

The main objective of this study is to understand better the interaction mechanism between a laminar boundary layer and an oblique shock that impinges on a wall or emerge from a compression corner.

## COMPUTATIONAL STUDY AND THE RESULTS

In this study, the computational simulations are performed using two different compressible Navier-Stokes solver, namely commercial software FLUENT and open source solver OpenFOAM. The adaptive mesh refinement capabilities and various upwind schemes of the solvers make them good candidates for the solution of SWBLI problem. This manuscript contains preliminary results of the Computational Fluid Dynamics (CFD) simulations for interactions of the shock wave / laminar boundary layers formed on a flat plate and a compression corner.

### SWBLI on a Compression Corner

A compressible flow over a compression corner that has a deflection angle of  $30^\circ$  is simulated here for comparison (see the Figure 2. below). The computational domain consist of 3 blocks. While the borders of the blocks are represented by thin black lines, the adiabatic walls at the bottom sections of the Block 1 and 2 are depicted by thick black lines. The Blocks 1, 2 and 3 have  $10 \times 100$ ,  $80 \times 100$ , and  $90 \times 100$  grid points in the horizontal and vertical directions, respectively. A uniform flow with a free stream Mach number of 10.30 enters the Block 1 from the left (Side AF), and then reaches the flat plate at point B. Finally, the flow turns into itself at the compression corner C, and then leaves the flow field from the side GE. The local Reynolds number at point C is equal to 24626. Relative lengths of the sides of the blocks are tabulated in Table 1.

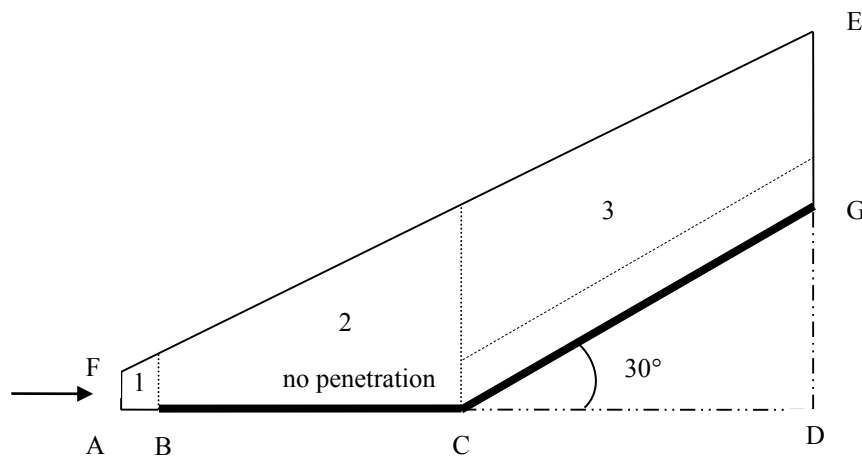


Figure 2: *Computational domain for SWBLI on a compression corner*

Table 1. Detail of the computational domain

AB	BC	CD	DG	GE	AF
0.5	4.004	4.657	2.689	2.311	0.5

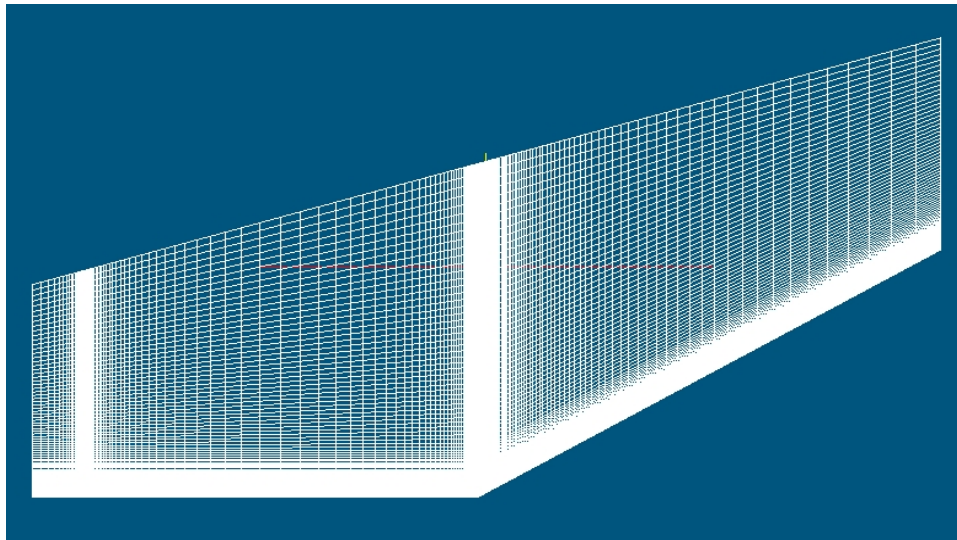


Figure 3: *Computational domain for SWBLI over a compression corner*

The grid used in the computations is shown in Figure 3. It consists of 27000 cells. The Mach contours and streamline plots of the present study and those are shown for comparison by Bono et al. (2008). As can be seen from the figure, although the disassociation of the air molecules are not considered in the present study, the results are qualitatively similar.

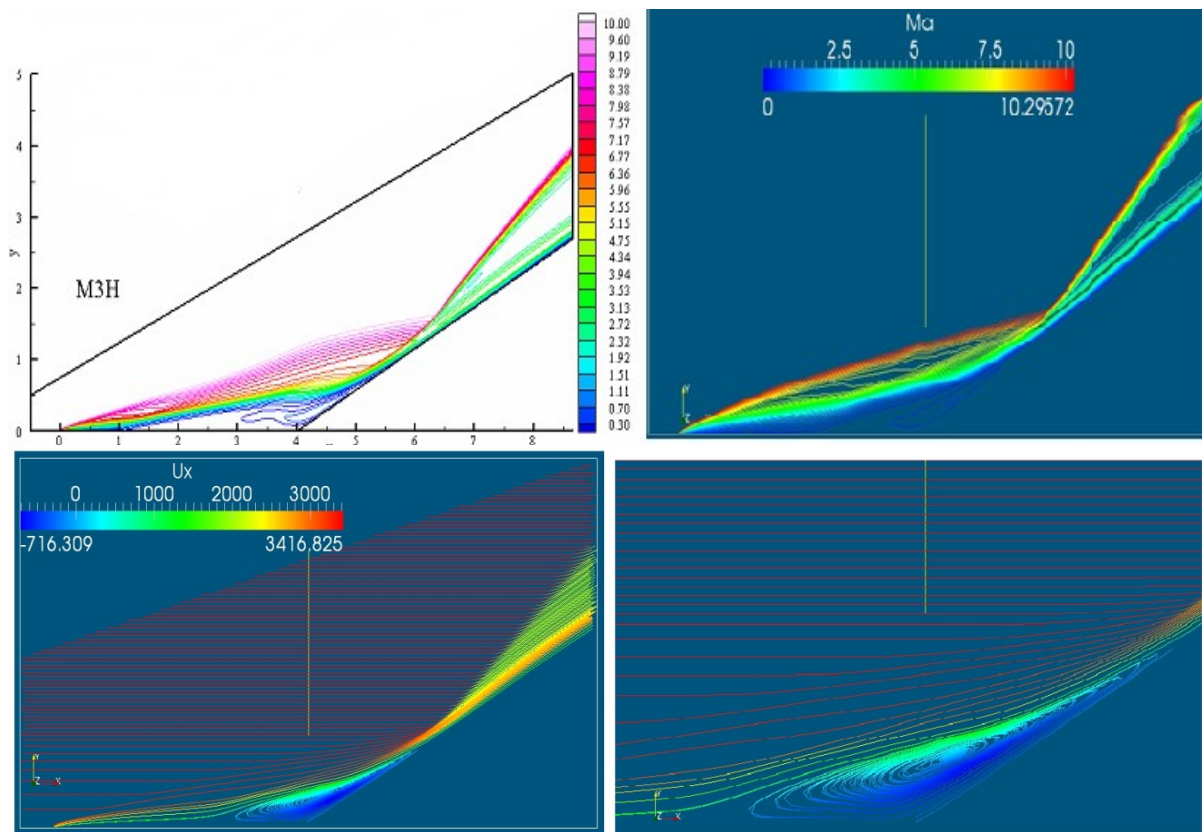


Figure 4: *Mach contours (top) and streamlines (bottom) for SWBLI over a compression corner*

The pressure coefficient variation along the adiabatic wall is calculated and then plotted in Figure 5 for comparison with the experimental and numerical studies by Bono et al. (2008) and Holden et al. (2006), respectively. Although the present study and the other numerical study is able to capture the trend quite well up to the compression corner, experimental result has significantly lower values than the numerical studies beyond the compression corner point.

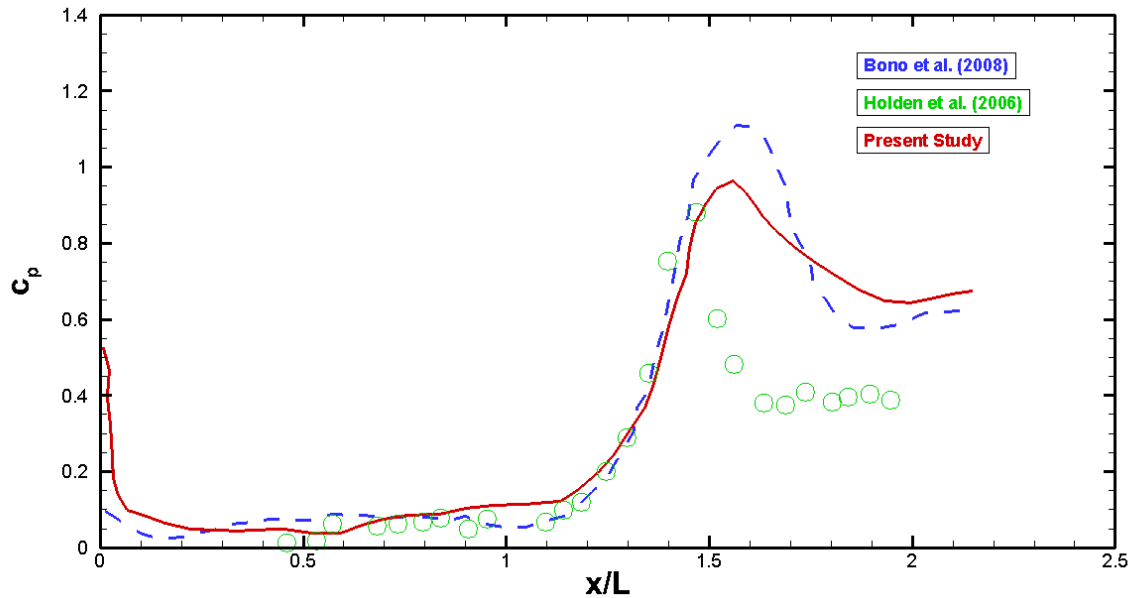


Figure 5: Comparison of the computational and analytical results in terms of Mach number variation

### SWBLI on a Flat Plate

Another flow configuration studied here is a Mach 2.15 flow entering a converging channel which is depicted in Figure 6. The inclination of the top wall of the nozzle with respect to the bottom one generates an oblique shock that impinges on the flat plate. This problem has been studied before by Degrez et al. (1987) numerically and experimentally. The geometrical details of the problem are tabulated in Table 2, where the lengths are normalized by the distance from the beginning of the flat plate to the point, where the shock wave impinges on the plate. The boundary conditions are set to simulate the experiment, where a Mach 2.15 flow with a stagnation pressure of  $1.07 \times 10^7$  Pa and total temperature of 293 K reaches the shock impingement point, where the local Reynolds number equal to  $10^5$ .

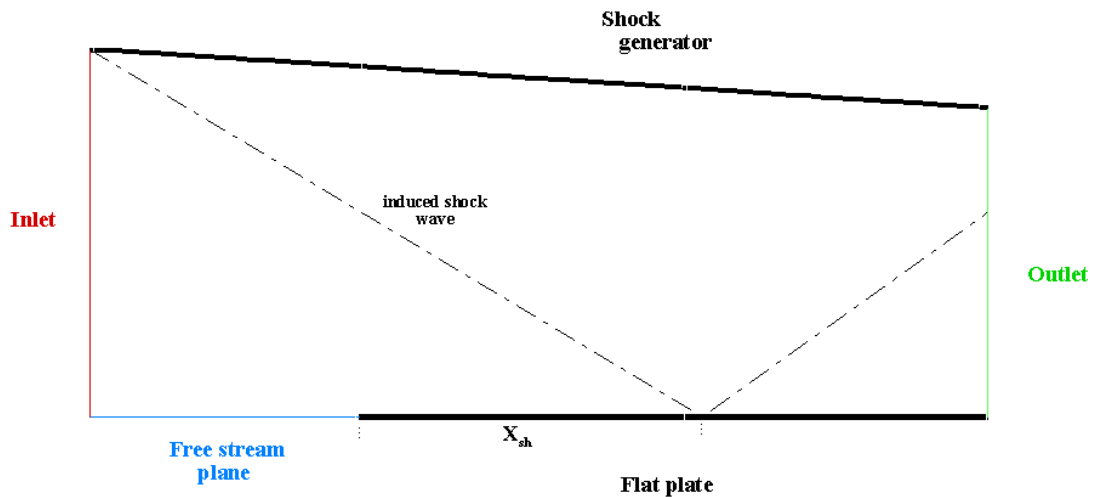


Figure 6: *Computational domain and the boundary conditions*

Table 2. Geometrical details of channel

Height of Inlet	Length of free stream plane	Length of flat plate	Inclination Angle [°]
1.125	0.775	2.034	3.75

A finite volume based commercial Navier-Stokes solver, ANSYS Fluent is used in the simulations. A density-based solver with a second-order upwind scheme is chosen for discretization. Besides, Advection Upstream Splitting Method (AUSM) is chosen for flux calculation. AUSM gives free of oscillations in the case of stationary and moving shock waves.

The computational domain consist of three blocks of structured quadrilateral meshes as can be seen from Figure 7. The whole domain consists of 24750 cells and the grid is refined at the stagnation point of the flat plate and shock impingement point, the region next to the inlet and outlet, and within the boundary layers formed on the upper and lower walls.

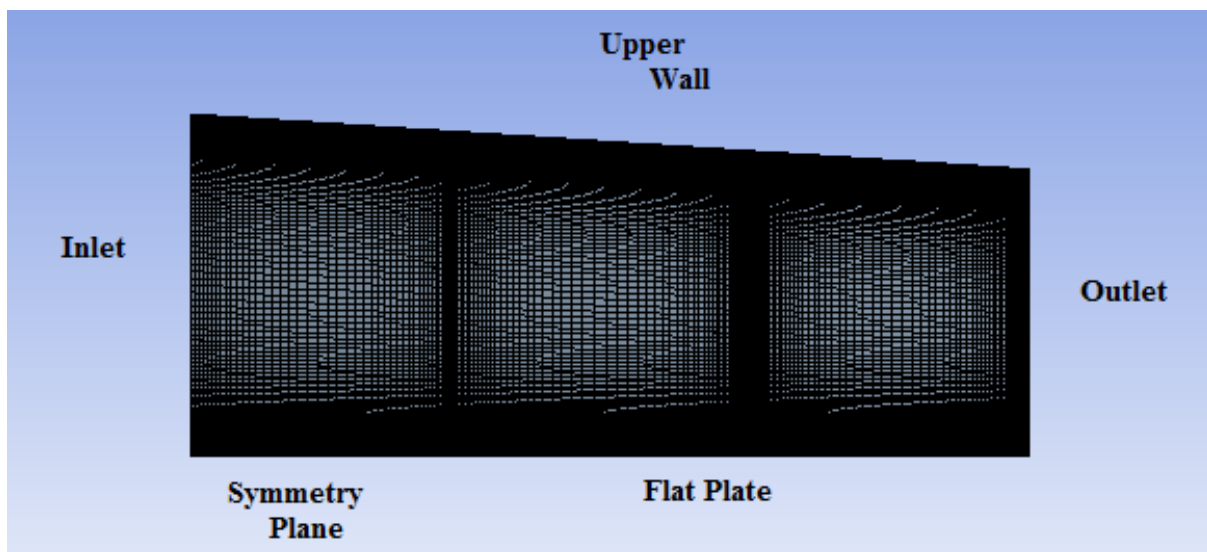


Figure 7: *The mesh used in the computations*

The pressure contours obtained for the test case are shown in Figure 8. As can be seen from the figure, the solver is able to capture the weak and the strong shock waves formed at the beginnings of the flat plate and the upper wall, the first and the second reflected shock waves, and the expansion fan.

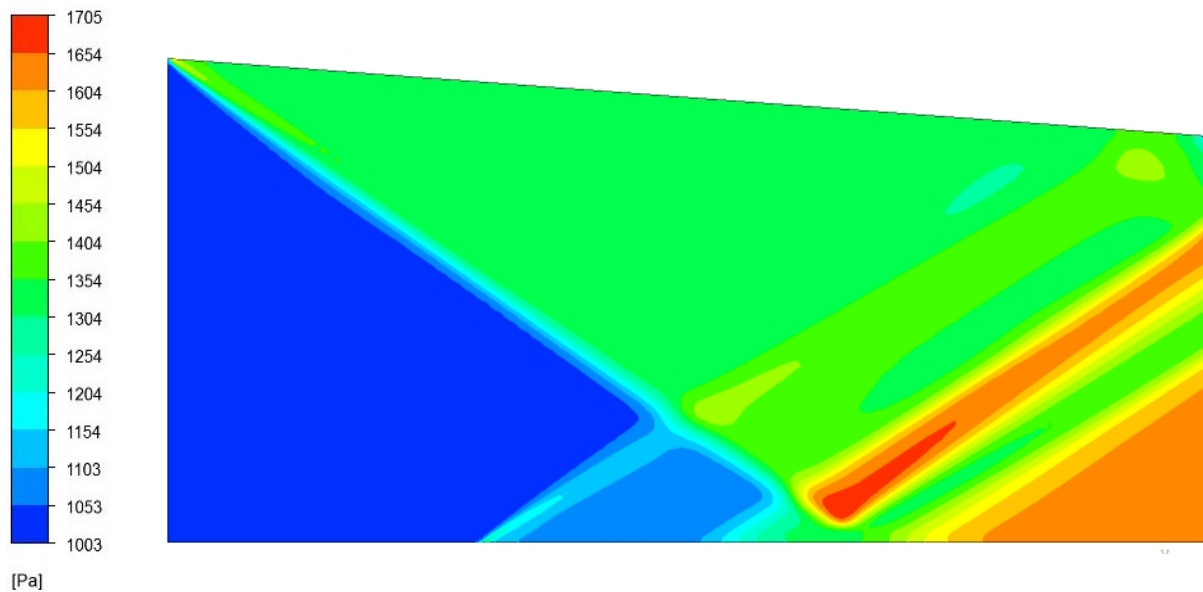


Figure 8: *Pressure contours obtained for the flow with  $\theta=3.75^\circ$*

In order to make a quantitative comparison, variation of pressure along the flat plate is plotted alongside the numerical and experimental results by Degrez et al. (1987) in Figure 9. As can be seen from the figure, the computational results are in good agreement with the Reference values. The discrepancies between the presented result and the others may result from the uncertainties in the experimental setup as described in the reference.

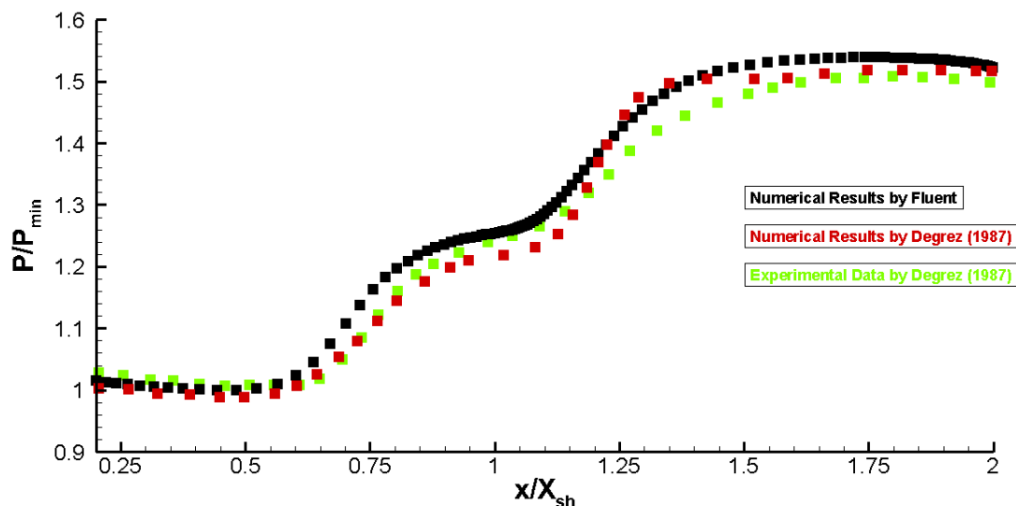


Figure 9: *Comparison of the pressure distribution along the flat plate*

A systematic study is performed to observe the effect of the shock impingement angle on the flow physics. As the inclination angle of the top wall is varied, the distance from the beginning of the flat plate to the impingement point of the resulting shock wave is kept the same to preserve the Reynolds number at the interaction point. In Figure 10, the thickening boundary layers because of shock impingement are represented for the deflection angles that is in the range of  $\theta=4^\circ$ - $12^\circ$ . As can be seen from the figure, as the deflection angle increases (in the direction of from top to bottom and from left to right), the boundary

layer gets thicker around the impingement point. The dotted and dashed lines shown in the figure represent the boundary layer and the sonic line, respectively. As the impingement angle increases, the separation bubble formed in the boundary layer gets wider and taller. At  $\theta=7^\circ$ , an additional separation bubble begins to form next to the wall in the interaction region. Then, as the shock impingement angle is increased, the number and the size of the separation bubbles are increased. As a result of thickening boundary layer, the expansion fan emerging from the impingement point gets stronger and the discontinuities in the pressure contours resulted from first and the second reflected shocks become more significant.

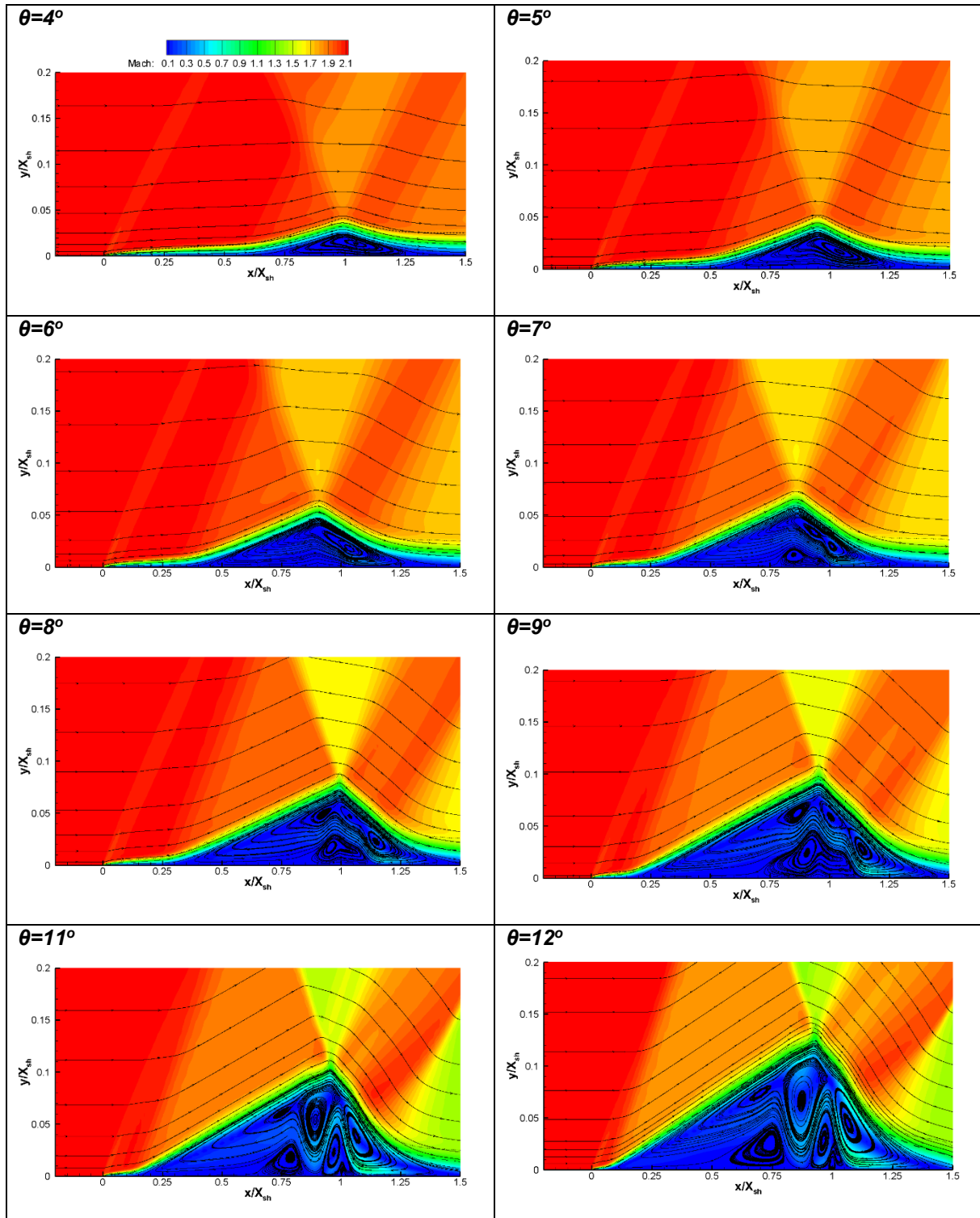


Figure 10: Close-up views of the interaction zones for  $\theta=4^\circ-12^\circ$

As described in the Introduction, when an oblique shock impinges on a laminar boundary layer formed on a flat plate, the flow separates from and then reattaches to the wall in the vicinity of the impingement point. In order to see the effects of shock impingement angle on the separation, the variations of wall skin friction coefficients around the shock impingement point for the cases with  $\theta=4^\circ-7^\circ$  are shown in Figure 11 for comparison. Starting from the beginning of the flat plate ( $x/X_{sh}=0$ ), the skin friction coefficients continuously decrease and then reach zero, where the separation from the wall takes place. As can be seen from the figure, the higher the deflection angle  $\theta$ , the longer the distance between the separation and the impingement point ( $x/X_{sh}=1.0$ ). The reattachment point is the location, where the skin friction coefficient reaches to zero after the impingement point. The reattachment points for the considered cases are almost the same at about  $x/X_{sh}=1.35$ . The appearance of the additional separation bubble observed in Figure 10 can also be seen from Figure 11, where the skin friction coefficient takes positive values between the separation and reattachment point for  $\theta=7^\circ$ .

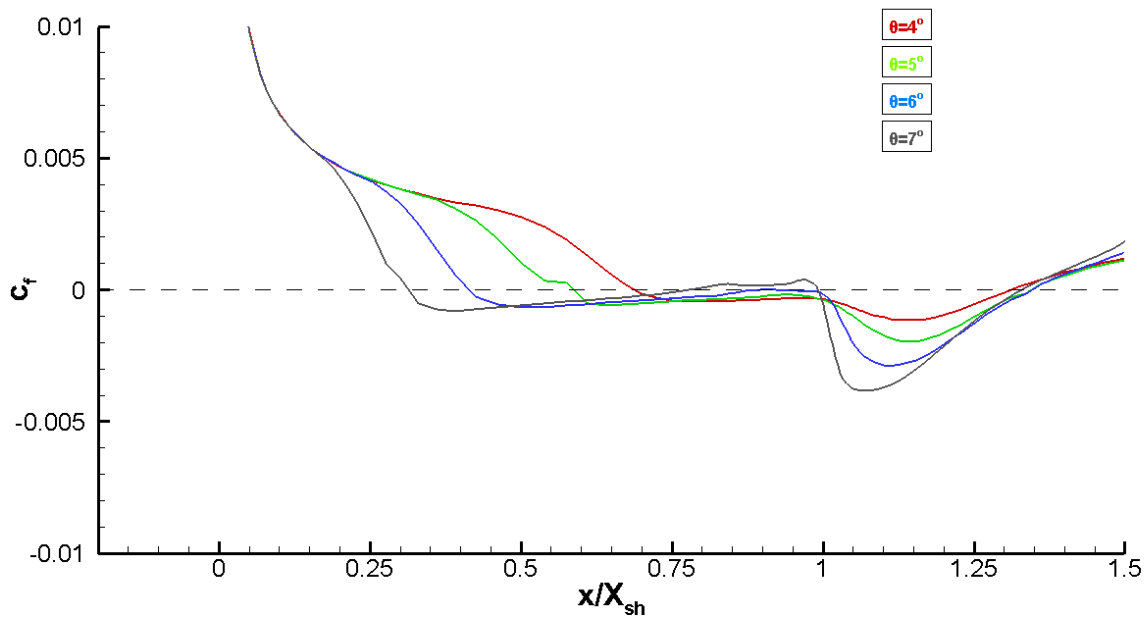


Figure 11: Variation of wall skin friction coefficient around the shock impingement point for  $\theta=4^\circ-7^\circ$

### FUTURE STUDIES

All the simulations presented here are obtained utilizing 2-dimensional, unsteady, compressible Navier-Stokes solvers. The complex flow physics observed in the interaction regime may require 3-dimensional unsteady flow simulations for the SWBLI flows with high impingement angle. The results of a recent study by Boin et al. (2006) reports that the flow becomes 3-dimensional for the impingement angle higher than  $35^\circ$ .

## References

- Boin, J.-Ph., Robinet, J.-Ch., Corre, Ch., and Deniau, H. (2006) *3D Steady and Unsteady Bifurcations in a Shock-Wave/Laminar Boundary Layer Interaction: A Numerical Study*, Theor. Comput. Fluid Dyn. Vol. 20, pp. 163-180 May 2006
- Bono, G., Awruch, A.M., and Popiolek, T.L. (2008) *Computational Study of Laminar Shock / Boundary Layer Interaction at Hypersonic Speeds*. Asociacion Argentina de Mecanica Computational. Vol. XXVII. 3135-3150 Nov 2008.
- Degrez, G., Boccadoro C.H., and Wendt J.F. (1987) *The Interaction of an Oblique Shock Wave with a Laminar Boundary Layer Revisited. An Experimental and Numerical Study*, J. Fluid Mech. Vol. 177, pp. 247-263 Apr 1987.
- Robinet, J.-Ch., Daru, V., and Tenaud, Ch. (n.d.) *Two-Dimensional Laminar Shock Wave / Boundary Layer Interaction*, SIMUNEF Laboratory, ENSAM-PARIS
- Pirozzoli, S., Beer, A., Bernardi, M., and Grasso, F. (2009) *Computational Analysis of Impinging Shock-Wave Boundary Layer Interaction under Conditions of Incipient Separation*, Shock Waves 19:487-497 July 2009
- Bertin, J.J., Cumings R.M. (2008) *Aerodynamics for Engineers*. Fifth edn. United States of America: Pearson Prentice Hall.
- Anderson, J.D. (2011) *Fundamentals of Aerodynamics*. Fifth edn. New York: McGraw-Hill.
- Delery, J.M. (2000) *Handbook of Shock Waves, Three Volume Set*. First edn. Academic Press, Vol 1.
- Houghton E.L., Carpenter P.W. (2012) *Aerodynamics for Engineering Students*, Sixth ed. Butterworth-Heinemann.
- Holden, M.S., Waldhams T.P., Harvey J.K. and Candler G.V. (2006) *Comparison between Measurements in Regions of Laminar Shock Wave Boundary Layer Interaction in Hypersonic Flows with Navier-Stokes and DSMC Solutions*, RTO-TR-AVT-007-V3.